JACS
JOURNAL OF THE AMERICAN CHEMICAL SOCIETY
pubs.acs.org/JACS
Communication

A Crystalline 1D Dynamic Covalent Polymer

Elisabet De Bolòs, Marta Martínez-Abadía, Félix Hernández-Culebras, Alison Haymaker, Kyle Swain, Karol Strutyński, Benjamin L. Weare, Javier Castells-Gil, Natalia M. Padial, Carlos Martí-Gastaldo, Andrei N. Khlobystov, Akinori Saeki, Manuel Melle-Franco, Brent L. Nannenga, and Aurelio Mateo-Alonso*

Cite This: J. Am. Chem. Soc. 2022, 144, 15443−15450
Read Online
ACCESS | Metrics & More | Article Recommendations | Supporting Information

ABSTRACT: The synthesis of crystalline one-dimensional polymers provides a fundamental understanding about the structure−property relationship in polymeric materials and allows the preparation of materials with enhanced thermal, mechanical, and conducting properties. However, the synthesis of crystalline one-dimensional polymers remains a challenge because polymers tend to adopt amorphous or semicrystalline phases. Herein, we report the synthesis of a crystalline one-dimensional polymer in solution by dynamic covalent chemistry. The structure of the polymer has been unambiguously confirmed by microcrystal electron diffraction that together with charge transport studies and theoretical calculations show how the π-stacked chains of the polymer generate optimal channels for charge transport.

Synthetic polymers are essential materials in modern society. The thermal, mechanical, and conducting properties of polymeric materials depend directly on their degree of crystallinity. The preparation of crystalline one-dimensional (1D) polymers remains a challenge in chemistry because polymers tend to adopt amorphous or semicrystalline phases constituted of entangled polymer chains. The availability of crystalline polymers enables a fundamental understanding of their structure−property relationship but also opens the door for the preparation of new materials with enhanced properties.[1] Topological polymerization has been used to obtain single crystals of 1D polymers.[2−10] This is a crystal-to-crystal transformation in which monomers that have been preorganized in a crystal lattice undergo a solid-state polymerization reaction. The scope of topological polymerization is limited because the precursors must be crystallized and carefully arranged in the lattice for the polymerization to take place. The synthesis of crystalline 1D polymers in solution or in dispersed media has a much broader scope. However, the synthesis of crystalline 1D polymers in solution is quite challenging because of their high degree of conformational freedom in solution, which makes the organization of the polymer chains across the three dimensions of a crystalline solid difficult.

Dynamic covalent chemistry has shown great success in the solution synthesis of crystalline organic materials with different dimensionality, such as 1D,[11,12] 2D,[13,14] and 3D[13,15] covalent organic frameworks. Under dynamic covalent chemistry conditions, the covalent bonds between the monomers can be formed and broken; hence, any structural error can be corrected by thermodynamic control. Approaches that combine dynamic covalent chemistry with templating motifs that limit the degrees of freedom of 1D polymers (e.g., coordination and hydrogen bonding) have been successfully used to weave,[16] stiffen,[17,18] and entwine[19] polymer chains into crystalline superstructures. Yet, despite these impressive advances, the synthesis of disentangled crystalline 1D polymers from solution remains elusive.[1,18,20]

Herein, we report the synthesis of a disentangled and highly crystalline 1D dynamic covalent polymer (**Bet-P-1**, where Bet stands for Elisabet) in solution. **Bet-P-1** has been obtained by the substoichiometric (1:1) linkage of tetratopic and ditopic building blocks (respectively compounds **1** and **2**, Figure 1a) through reversible imine bonds. The crystal structure of **Bet-P-1** has been solved by microcrystal electron diffraction (MicroED) and shows that the disentangled polymer chains are tightly packed by π-stacking (Figure 1b−e). Electronic absorption and charge transport studies combined with theoretical investigations show that such interchain π-stacking opens up optimal channels for charge transport.

We selected dibenzotetraazahexacene derivatives as nodes because of their synthetic accessibility, versatility, enhanced stability, and tendency to self-assemble by π-stacking.[21] Dibenzotetraazahexacene **1** was synthesized in two steps from 2,7-di-*tert*-butyl-4,5,9,10-pyrenetetraone (**3**) (Scheme 1). First, condensation of pyrenetetraone **3**[22] with 2.1 equiv of 4,5-dibromo-1,2-phenylenediamine (**4**) in acetic acid yielded tetrabromodibenzotetraazahexacene **5** (95%) as a highly insoluble yellow solid that could be characterized only by ^{1}H NMR in deuterated trifluoroacetic acid (TFA-d_1) and MS. Then, Suzuki coupling between tetrabromodibenzotetraazahexacene **5** and 4-formylphenylboronic acid (**6**) yielded

Received: June 19, 2022
Published: August 22, 2022

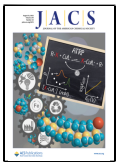

https://doi.org/10.1021/jacs.2c06446
J. Am. Chem. Soc. 2022, 144, 15443−15450

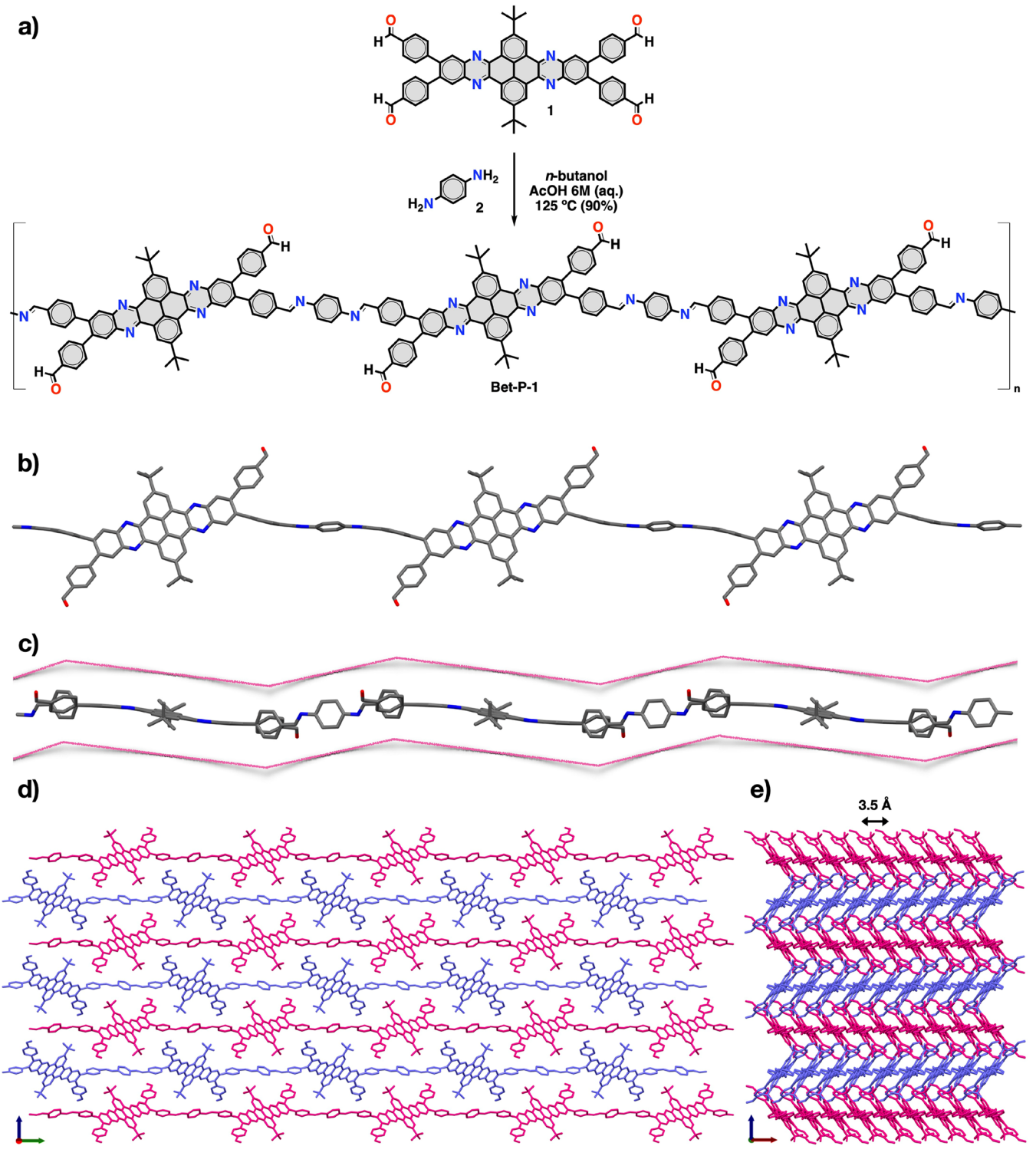

Figure 1. (a) Synthetic route for **Bet-P-1**. (b) Front and (c) side views of a single chain of **Bet-P-1** in the crystal structure. (d) Top and (e) side views of the crystal structure of **Bet-P-1** illustrating the packing of the different chains. Double arrow in the panel indicates the distance between the neighboring dibenzotetraazahexacene units. Hydrogens have been omitted for clarity.

dibenzotetraazahexacene **1** (22%) as an orangish solid that shows an optimal solubility for solution synthesis.

Initially, we screened several conditions for the condensation of dibenzotetraazahexacene **1** with *p*-phenylenediamine (**2**) in different solvent mixtures (*o*-dichlorobenzene, mesitylene, and *n*-butanol), different concentrations of aqueous acetic acid, and different stoichiometries (1:1, 1:2, 1:4). We used powder X-ray diffraction (PXRD) of the isolated solids to select the best conditions to obtain crystalline materials. Based on the screening experiments (a selection is shown in Figure S1), orangish crystalline powders of **Bet-P-1** were prepared in a 90% yield by condensation of a 1:2 molar mixture of dibenzotetraazahexacene **1** and *p*-phenylenediamine (**2**) in *n*-butanol in the presence of a 6 M aqueous solution of acetic

https://doi.org/10.1021/jacs.2c06446
J. Am. Chem. Soc. 2022, 144, 15443−15450

Scheme 1. Synthesis of Precursor 1

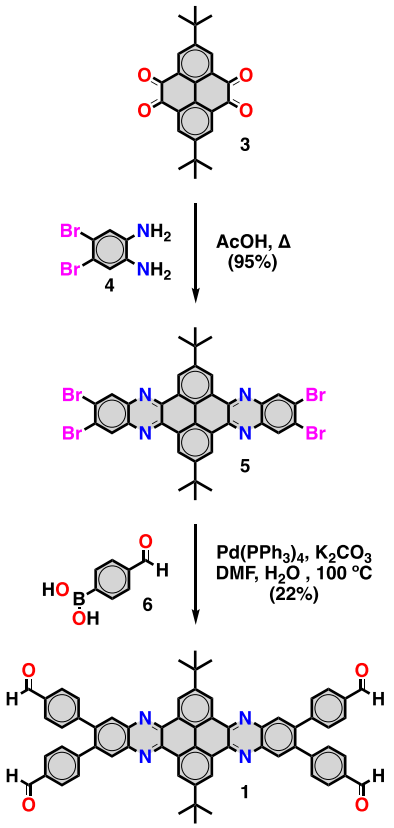

acid (Figure 1a). Similarly to imine-linked covalent organic frameworks (COFs), **Bet-P-1** crystals show no sign of decomposition in nonprotic solvents such as acetone, chloroform, and hexane. Thermal gravimetric analysis under N_2 shows that **Bet-P-1** is stable up to ∼500 °C (Figure S2).

The PXRD pattern of **Bet-P-1** suggests the formation of a highly crystalline material with a large number of sharp, well-resolved X-ray reflections (Figure 2a). Field emission scanning electron microscopy (FE-SEM) and high-resolution transmission electron microscopy (HR-TEM) show that the powders of **Bet-P-1** are constituted by needle-like microcrystals with the typical length of ca. 10 μm and diameters between 100 and 300 nm (Figures 2b, S3, and S4). FE-SEM imaging of surfaces of individual crystals indicated a helical twist of the crystal facets (Figure S3). High-magnification HR-TEM imaging of individual crystals reveals the presence of distinct lattice fringes that are separated by a distance of 1.4 nm running parallel to the main axis of the crystal (Figures 2c–e and S5 and S6). This further confirms the high crystallinity and also illustrates the dense packing of polymeric chains in **Bet-P-1**. This dense packing is also consistent with the nitrogen uptake measurements that show a virtually negligible adsorption and a very low Brunauer–Emmett–Teller (BET) surface area of 11 $m^2\ g^{-1}$ (Figure 2f). For instance, the Zeo++ and Poreblazer surface areas calculated for the crystal structure of **Bet-P-1** are 0 $m^2\ g^{-1}$ in both cases.

Although, theoretically, a 2D COF can be formed from a 1:2 molar ratio of dibenzotetraazahexacene **1** and *p*-phenylenediamine (**2**), the spectroscopic characterization shows that only two pairs of aldehydes were transformed into imines, generating a copolymer in 1:1 molar ratio. For instance, the Fourier transformed infrared (FT-IR) spectrum of **Bet-P-1** shows the imine C═N stretch band (1619 cm^{-1}), whereas the aldehyde C═O stretch band (1701 cm^{-1}) does not show any signs of attenuation (Figure 2g). This is in agreement with the cross-polarization/magic angle spinning (CP/MAS) solid-state ^{13}C nuclear magnetic resonance (NMR) spectrum of **Bet-P-1**, which exhibited two signals that correspond respectively to the imine and to the unreacted aldehyde groups (Figure 2h). Additionally, the NMR spectrum of the hydrolysis/digestion of the **Bet-P-1** crystalline powders in TFA-d_1 shows the signals of the hydrolyzed dibenzotetraazahexacene **1** and *p*-phenylenediamine (**2**) monomers in a precise 1:1 ratio (Figure 2i), in agreement with the 1:1 stoichiometry of the polymer, including some residual peaks of the solvents used during filtration such as acetone and hexane.

The crystal structure of **Bet-P-1** was solved by MicroED[23] with data from four crystals at a specimen temperature of ∼100 K that were collected and merged together to produce a final refined structure at 0.80 Å with the $P2_1/n$ space group (Figure 1b–e; Table S1). The theoretical PXRD pattern of the crystal structure of **Bet-P-1** determined by MicroED shows an excellent correlation with the experimental PXRD pattern (Figure 2a). We used the Pawley refinement of the experimental PXRD pattern of the bulk material versus the monoclinic crystal structure of **Bet-P-1** determined by MicroED to confirm phase purity with excellent agreement factors (a = 6.18 Å, b = 16.36 Å, c = 26.58 Å, R_{wp}= 2.39%, and R_p= 1.67%) (Figure 2a; Table S2). The crystal structure unambiguously confirms that **Bet-P-1** is a linear polymer with a 1:1 molar ratio of monomers (Figure 1b,c), in which the dibenzotetraazahexacene nodes are covalently bound to the *p*-phenylenediamine linkers by two imines in a transoid configuration, leaving two unreacted aldehyde groups. **Bet-P-1** adopts a staircase-shaped conformation along the imine backbone (Figure 1c), where the 4-formylphenyl and the (4-formylphenyl)imino substituents are out of the plane of the dibenzotetraazahexacene nodes by 32° and 74°, respectively. The staircase-shaped linear polymer chains of **Bet-P-1** are π-stacked on top of each other at a distance of 3.5 Å (Figure 1e). These π-stacks crystallize in an antiparallel herringbone arrangement (Figure 1d), which gives rise to a densely packed crystal that is consistent with HR-TEM observations. For instance, the high contrast areas in the TEM micrographs correspond to the areas of highest density associated with the aromatic stacks of dibenzotetraazahexacene moieties, in particular in the (011) crystal planes (Figures 2c–e and S5 and S6). Based on the crystal structure of **Bet-P-1**, a potential rationale for the formation of a 1D polymer instead of a COF could be the excellent complementarity of the staircase-shaped linear polymer strands that act as polymeric docking sites, similarly to what was previously described for COFs obtained from stackable monomers.[24−27]

To shine some light on the optoelectronic properties of **Bet-P-1**, the solid-state UV–vis–NIR electronic absorption spectrum was compared with that of dibenzotetraazahexacene **1** (Figure 3a). The absorption spectrum of **Bet-P-1** shows absorption bands similar to that of dibenzotetraazahexacene **1** but slightly red-shifted, which is consistent with a more extensive π-stacking. The optical band gap of **Bet-P-1** estimated according to the Kubelka–Munk-transformed reflectance spectrum corresponds to 2.6 eV (inset Figure 3a).

To provide additional insights on the electronic structure and the charge-transporting properties of the microcrystals of **Bet-P-1**, we performed density functional theory (DFT) solid-

https://doi.org/10.1021/jacs.2c06446
J. Am. Chem. Soc. 2022, 144, 15443−15450

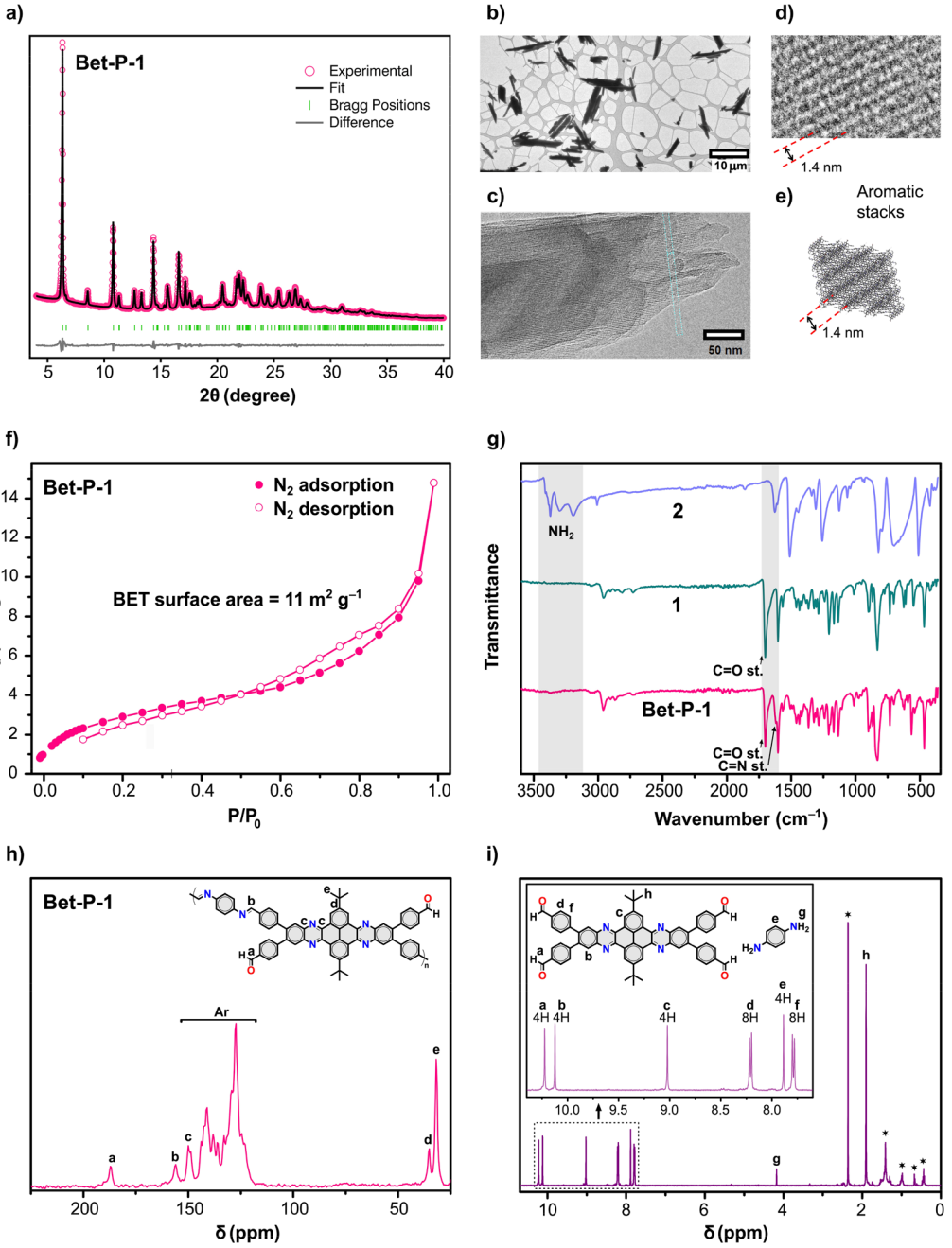

Figure 2. (a) Pawley refinement of the experimental diffraction data of **Bet-P-1** collected at room temperature. (b) Large field of view 200 kV TEM image of needle-like crystals dispersed on a lacey-carbon-coated grid. (c) HR-TEM image of an individual crystal revealing distinct lattice fringes running along the main axis of the crystal. (d, e) Separation of 1.4 nm between the areas of high contrast indicating aromatic moieties of the polymer forming (011) crystal planes. (f) N_2 adsorption and desorption curves for **Bet-P-1**. (g) FT-IR spectra of *p*-phenylenediamine, **1**, and **Bet-P-1**. (h) CP/MAS ^{13}C NMR spectrum of **Bet-P-1**. (i) ^{1}H NMR spectrum of a hydrolyzed **Bet-P-1** sample in TFA-d_1 showing the signals of dibenzotetraazahexacene **1** and *p*-phenylenediamine (**2**) monomers (*indicates solvent residual peak).

state calculations with the PBE functional (details in the Supporting Information). The computed electronic band structure shows that **Bet-P-1** crystals are direct gap semiconductors with a band gap of 1.79 eV at the D-point (0.5 0.0 0.5) (Figure 3b). The highest occupied crystalline orbital (HOCO) band shows a weak bandwidth (40 meV), while the lowest unoccupied crystalline orbital (LUCO) band shows an increased bandwidth (120 meV), which can be mostly attributed to $\pi-\pi$ stacking (see below). In addition, for increased accuracy, we also computed the band gap with the B3LYP hybrid functional, which yielded a value of 2.95 eV, similar to the band gap estimated experimentally. The frontier orbitals were analyzed in a 2×2×2 supercell computed in real space (details in the Supporting Information). In this system, the degenerate HOCOs show a localized electronic density on the phenylenebisphenylmethanimine residues (Figures 3c and S7), whereas the degenerate LUCOs show a localized electronic density on the dibenzotetraazahexacene nodes (Figures 3d and S7). Remarkably, due to the polymer intermolecular packing, the electron densities of some of the degenerate LUCOs spread throughout neighboring π-stacked dibenzotetraazahexacene units (Figure 3e), which opens up

https://doi.org/10.1021/jacs.2c06446
J. Am. Chem. Soc. 2022, 144, 15443−15450

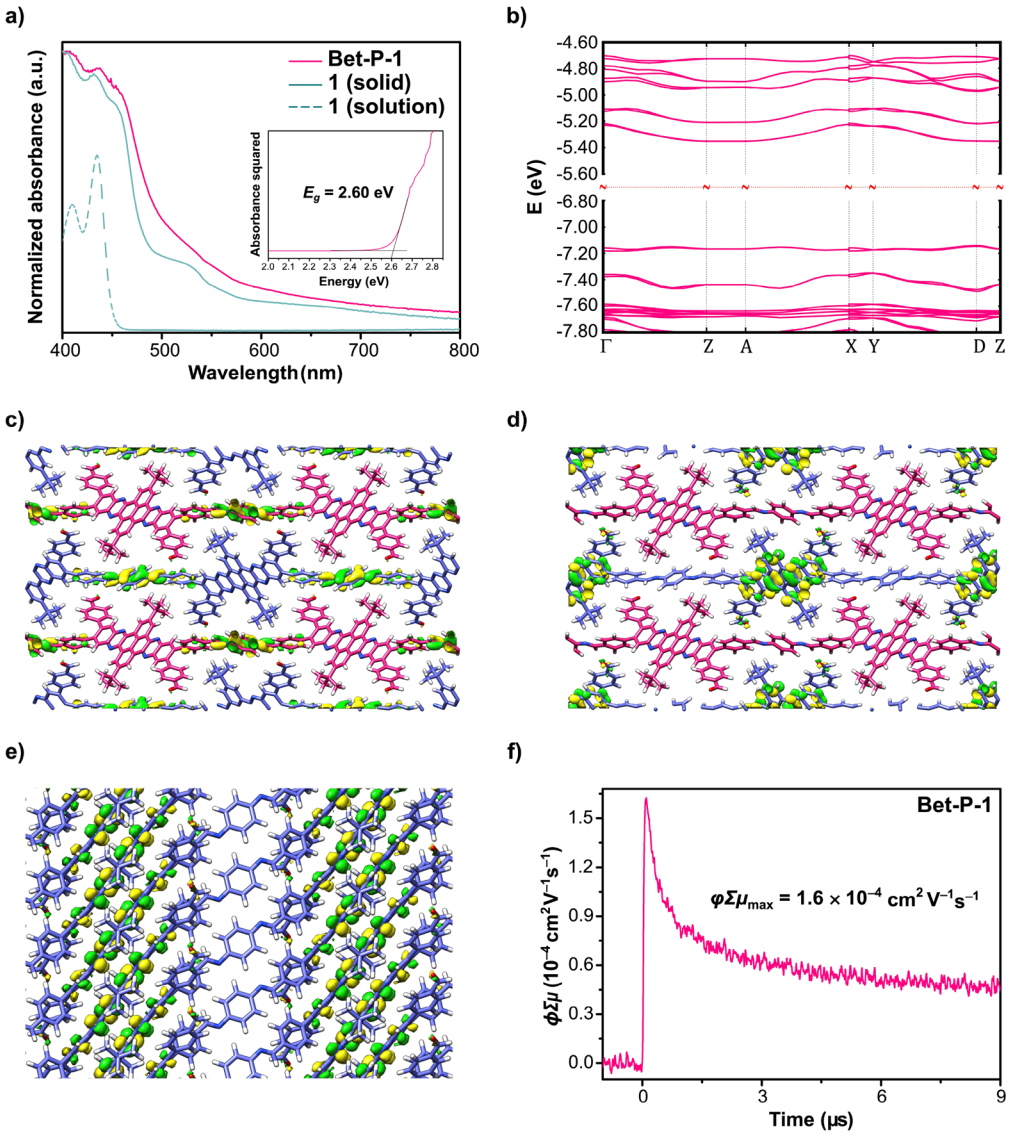

Figure 3. (a) UV−vis−NIR electronic absorption spectrum of **Bet-P-1**. The inset shows the estimated band gap. (b) Calculated band structure of the crystal structure of **Bet-P-1**. Top views of selected (c) HOCOs and (d) LUCOs of a **Bet-P-1** supercell. (e) Side view of the LUCO of a **Bet-P-1** supercell. (f) FP-TRMC conductivity transients of **Bet-P-1** upon excitation at 355 nm, 9.1 × 10^{15} photons cm^{-2} pulse^{-1}.

channels for electronic transport. To further confirm these channels, a detailed analysis of the bands was performed on a simplified unit cell representing a slab model of a 2D periodic system with an inclined unit cell sharing the same geometry of the bulk crystal but containing only one polymer strand parallel to the main unit cell axis with $\pi-\pi$ stacking on the second unit cell axis (Figure S8 and Table S3). This model also shows that the most dispersive frontier band is the LUCO on the π-stacking direction with a bandwidth of 106 meV.

The charge transport properties of the crystalline powders of **Bet-P-1** were investigated by flash-photolysis time-resolved microwave conductivity (FP-TRMC).[28] This technique measures the pseudophotoconductivity or the intrinsic charge carrier mobility ($\varphi\Sigma\mu$, where φ is the quantum yield and $\Sigma\mu$ is the sum of the charge carrier mobilities) directly on powders and films without the need of electrodes. FP-TRMC measurements on **Bet-P-1** show a maximum $\varphi\Sigma\mu$ value ($\varphi\Sigma\mu_{max}$) of 1.6 × 10^{-4} cm^2 V^{-1} s^{-1} (Figure 3f). This $\varphi\Sigma\mu_{max}$ value is in the same range as the values observed on other π-stacked conducting systems, such as stacked pseudorotaxanes,[29] supramolecular polymers,[30] π-gels,[31,32] covalent organic frameworks,[26,27,33−44] and fused-aromatic networks,[45] which show $\varphi\Sigma\mu_{max}$ values that oscillate between 10^{-5} and 10^{-4} cm^2 V^{-1} s^{-1}. The observed $\varphi\Sigma\mu_{max}$ value and the inter-macromolecular spread of the electronic densities at the LUCO indicate that electronic transport takes place preferentially across the channels generated by the π-stacked dibenzotetraazahexacene residues of **Bet-P-1**.

To conclude, we have described the successful solvothermal synthesis of a disentangled crystalline 1D polymer (**Bet-P-1**) by dynamic covalent chemistry. The structure of **Bet-P-1** has been unambiguously confirmed by MicroED and is consistent with PXRD, HR-TEM, porosimetry, FT-IR, and NMR characterization. The crystal structure shows that the extended chains of **Bet-P-1** are π-stacked to one another through the dibenzohexacene units, which opens up channels optimal for charge transport. For instance, UV−vis−NIR electronic absorption, FP-TRMC, and theoretical calculations illustrate that **Bet-P-1** is a direct gap semiconductor with an intrinsic charge carrier mobility comparable to that observed in state-of-

https://doi.org/10.1021/jacs.2c06446
J. Am. Chem. Soc. 2022, 144, 15443−15450

the-art π-stacked materials. This work illustrates that dynamic covalent chemistry is also a valuable tool for the synthesis of crystalline 1D polymers without the need of any templating strategy and paves the way for the synthesis of other families of crystalline 1D polymers with enhanced performance for electronic applications.

■ ASSOCIATED CONTENT

Supporting Information

The Supporting Information is available free of charge at https://pubs.acs.org/doi/10.1021/jacs.2c06446.

Experimental details of the synthesis, characterization, and calculations (PDF)

Accession Codes

CCDC 2177984 contains the supplementary crystallographic data for this paper. These data can be obtained free of charge via www.ccdc.cam.ac.uk/data_request/cif, or by emailing data_request@ccdc.cam.ac.uk, or by contacting The Cambridge Crystallographic Data Centre, 12 Union Road, Cambridge CB2 1EZ, UK; fax: +44 1223 336033.

■ AUTHOR INFORMATION

Corresponding Author

Aurelio Mateo-Alonso − *POLYMAT, University of the Basque Country UPV/EHU, Donostia-San Sebastián 20018, Spain; Ikerbasque, Basque Foundation for Science, Bilbao 48009, Spain;* orcid.org/0000-0002-5316-2594; Email: amateo@polymat.eu

Authors

Elisabet De Bolòs − *POLYMAT, University of the Basque Country UPV/EHU, Donostia-San Sebastián 20018, Spain*

Marta Martínez-Abadía − *POLYMAT, University of the Basque Country UPV/EHU, Donostia-San Sebastián 20018, Spain*

Félix Hernández-Culebras − *POLYMAT, University of the Basque Country UPV/EHU, Donostia-San Sebastián 20018, Spain*

Alison Haymaker − *Chemical Engineering, School for Engineering of Matter, Transport, and Energy, Arizona State University, Tempe, Arizona 85287, United States; Center for Applied Structural Discovery, The Biodesign Institute, Arizona State University, Tempe, Arizona 85281, United States*

Kyle Swain − *Chemical Engineering, School for Engineering of Matter, Transport, and Energy, Arizona State University, Tempe, Arizona 85287, United States; Center for Applied Structural Discovery, The Biodesign Institute, Arizona State University, Tempe, Arizona 85281, United States*

Karol Strutyński − *CICECO - Aveiro Institute of Materials, Department of Chemistry, University of Aveiro, Aveiro 3810-193, Portugal*

Benjamin L. Weare − *School of Chemistry, University of Nottingham, Nottingham NG7 2RD, United Kingdom;* orcid.org/0000-0003-4209-2604

Javier Castells-Gil − *Instituto de Ciencia Molecular, Universidad de Valencia, Paterna 46980, Spain*

Natalia M. Padial − *Instituto de Ciencia Molecular, Universidad de Valencia, Paterna 46980, Spain*

Carlos Martí-Gastaldo − *Instituto de Ciencia Molecular, Universidad de Valencia, Paterna 46980, Spain*

Andrei N. Khlobystov − *School of Chemistry, University of Nottingham, Nottingham NG7 2RD, United Kingdom; The Nanoscale and Microscale Research Centre, University of Nottingham, Nottingham NG7 2RD, United Kingdom;* orcid.org/0000-0001-7738-4098

Akinori Saeki − *Department of Applied Chemistry, Graduate School of Engineering, Osaka University, Suita, Osaka 565-0871, Japan;* orcid.org/0000-0001-7429-2200

Manuel Melle-Franco − *CICECO - Aveiro Institute of Materials, Department of Chemistry, University of Aveiro, Aveiro 3810-193, Portugal;* orcid.org/0000-0003-1929-0477

Brent L. Nannenga − *Chemical Engineering, School for Engineering of Matter, Transport, and Energy, Arizona State University, Tempe, Arizona 85287, United States; Center for Applied Structural Discovery, The Biodesign Institute, Arizona State University, Tempe, Arizona 85281, United States;* orcid.org/0000-0001-6859-3429

Complete contact information is available at: https://pubs.acs.org/10.1021/jacs.2c06446

Author Contributions

The manuscript was written through contributions of all authors. All authors have given approval to the final version of the manuscript.

Notes

The authors declare no competing financial interest.

■ ACKNOWLEDGMENTS

This work was carried out with support from the Basque Science Foundation for Science (Ikerbasque), POLYMAT, the University of the Basque Country, Diputación de Guipúzcoa, Gobierno Vasco (PIBA_2022_1_0031 and BERC program), Generalitat Valenciana (PROMETEU/2021/054) and Gobierno de España (Projects CEX2020-001067-M, PID2021-124484OB-I00,PID2020-118117RB-I00 and CEX2019-000919-M financed by MCIN/AEI/10.13039/501100011033). Project (PCI2022-132921) funded by the Agencia Estatal de Investigación through the PCI 2022 and M-ERA.NET 2021 calls. Technical and human support provided by SGIker of UPV/EHU and European funding (ERDF and ESF) is acknowledged. This project has received funding from the European Research Council (ERC) under the European Union's Horizon 2020 research and innovation program (Grant Agreement No. 722951 and 714122). This project has received funding from the European Union's Horizon 2020 research and innovation program under grant agreement No. 899895. This work was funded by the European Union under the Horizon Europe grant 101046231. This project has received support from the National Institutes of Health (R21GM135784) and the use of the Titan Krios within the Eyring Materials Center at Arizona State University (NSF DBI 1531991). Support through project IF/00894/2015 and within the scope of the project CICECO-Aveiro Institute of Materials, UIDB/50011/2020, UIDP/50011/2020 & LA/P/0006/2020, financed by national funds through the FCT/MEC (PIDDAC), is gratefully acknowledged. We thank the Nanoscale and Microscale Research Centre (nmRC), University of Nottingham, for access to EM instrumentation. N.M.P. thanks La Caixa Foundation for a Postdoctoral Junior Leader−Retaining Fellowship (ID 100010434 and fellowship code LCF/BQ/PR20/11770014).

REFERENCES

(1) Agbolaghi, S.; Abbaspoor, S.; Abbasi, F. A comprehensive review on polymer single crystals—From fundamental concepts to applications. *Prog. Polym. Sci.* **2018**, *81*, 22−79.

(2) Hasegawa, M.; Suzuki, Y. Four-center type photopolymerization in the solid state: Poly-2,5-distrylpyrazine. *J. Polym. Sci., Part B: Polym. Phys.* **1967**, *5* (9), 813−815.

(3) Wegner, G. Topochemische Reaktionen von Monomeren mit konjugierten Dreifachbindungen/Tochemical Reactions of Monomers with conjugated triple Bonds: I., Mitt.: Polymerisation von Derivaten des 2.4-Hexadiin-1.6-diols im kristallinen Zustand. *Naturforsch. B* **1969**, *24* (7), 824−832.

(4) Hasegawa, M., Photodimerization and Photopolymerization of Diolefin Crystals. In *Advances in Physical Organic Chemistry*; Bethell, D., Ed. Academic Press, 1995; Vol. *30*, pp 117−171.

(5) Matsumoto, A.; Tanaka, T.; Tsubouchi, T.; Tashiro, K.; Saragai, S.; Nakamoto, S. Crystal Engineering for Topochemical Polymerization of Muconic Esters Using Halogen-Halogen and CH/π Interactions as Weak Intermolecular Interactions. *J. Am. Chem. Soc.* **2002**, *124* (30), 8891−8902.

(6) Sun, A.; Lauher, J. W.; Goroff, N. S. Preparation of Poly(diiododiacetylene), an Ordered Conjugated Polymer of Carbon and Iodine. *Science* **2006**, *312* (5776), 1030−1034.

(7) Biradha, K.; Santra, R. Crystal engineering of topochemical solid state reactions. *Chem. Soc. Rev.* **2013**, *42* (3), 950−967.

(8) Dou, L.; Zheng, Y.; Shen, X.; Wu, G.; Fields, K.; Hsu, W.-C.; Zhou, H.; Yang, Y.; Wudl, F. Single-Crystal Linear Polymers Through Visible Light-Triggered Topochemical Quantitative Polymerization. *Science* **2014**, *343* (6168), 272−277.

(9) Krishnan, B. P.; Sureshan, K. M. A Spontaneous Single-Crystal-to-Single-Crystal Polymorphic Transition Involving Major Packing Changes. *J. Am. Chem. Soc.* **2015**, *137* (4), 1692−1696.

(10) Athiyarath, V.; Sureshan, K. M. Designed Synthesis of a 1D Polymer in Twist-Stacked Topology via Single-Crystal-to-Single-Crystal Polymerization. *Angew. Chem., Int. Ed.* **2020**, *59* (36), 15580−15585.

(11) Nguyen, H. L.; Gropp, C.; Yaghi, O. M. Reticulating 1D Ribbons into 2D Covalent Organic Frameworks by Imine and Imide Linkages. *J. Am. Chem. Soc.* **2020**, *142* (6), 2771−2776.

(12) Koner, K.; Karak, S.; Kandambeth, S.; Karak, S.; Thomas, N.; Leanza, L.; Perego, C.; Pesce, L.; Capelli, R.; Moun, M.; Bhakar, M.; Ajithkumar, T. G.; Pavan, G. M.; Banerjee, R. Porous covalent organic nanotubes and their assembly in loops and toroids. *Nat. Chem.* **2022**, *14* (5), 507−514.

(13) Diercks, C. S.; Yaghi, O. M. The atom, the molecule, and the covalent organic framework. *Science* **2017**, *355* (6328), No. eaal1585.

(14) Martínez-Abadía, M.; Mateo-Alonso, A. Structural Approaches to Control Interlayer Interactions in 2D Covalent Organic Frameworks. *Adv. Mater.* **2020**, *32* (40), 2002366.

(15) Guan, X.; Chen, F.; Fang, Q.; Qiu, S. Design and applications of three dimensional covalent organic frameworks. *Chem. Soc. Rev.* **2020**, *49* (5), 1357−1384.

(16) Liu, Y.; Ma, Y.; Zhao, Y.; Sun, X.; Gándara, F.; Furukawa, H.; Liu, Z.; Zhu, H.; Zhu, C.; Suenaga, K.; Oleynikov, P.; Alshammari, A. S.; Zhang, X.; Terasaki, O.; Yaghi, O. M. Weaving of organic threads into a crystalline covalent organic framework. *Science* **2016**, *351* (6271), 365−369.

(17) Xu, H.-S.; Luo, Y.; Li, X.; See, P. Z.; Chen, Z.; Ma, T.; Liang, L.; Leng, K.; Abdelwahab, I.; Wang, L.; Li, R.; Shi, X.; Zhou, Y.; Lu, X. F.; Zhao, X.; Liu, C.; Sun, J.; Loh, K. P. Single crystal of a one-dimensional metallo-covalent organic framework. *Nat. Commun.* **2020**, *11* (1), 1434.

(18) Xu, H.-S.; Luo, Y.; See, P. Z.; Li, X.; Chen, Z.; Zhou, Y.; Zhao, X.; Leng, K.; Park, I.-H.; Li, R.; Liu, C.; Chen, F.; Xi, S.; Sun, J.; Loh, K. P. Divergent Chemistry Paths for 3D and 1D Metallo-Covalent Organic Frameworks (COFs). *Angew. Chem., Int. Ed.* **2020**, *59* (28), 11527−11532.

(19) Hu, Y.; Teat, S. J.; Gong, W.; Zhou, Z.; Jin, Y.; Chen, H.; Wu, J.; Cui, Y.; Jiang, T.; Cheng, X.; Zhang, W. Single crystals of mechanically entwined helical covalent polymers. *Nat. Chem.* **2021**, *13* (7), 660−665.

(20) Vodak, D. T.; Braun, M.; Iordanidis, L.; Plévert, J.; Stevens, M.; Beck, L.; Spence, J. C. H.; O'Keeffe, M.; Yaghi, O. M. One-Step Synthesis and Structure of an Oligo(spiro-orthocarbonate). *J. Am. Chem. Soc.* **2002**, *124* (18), 4942−4943.

(21) Mateo-Alonso, A. Pyrene-fused pyrazaacenes: from small molecules to nanoribbons. *Chem. Soc. Rev.* **2014**, *43* (17), 6311−6324.

(22) El-Assaad, T. H.; Parida, K. N.; Cesario, M. F.; McGrath, D. V. Sterically driven metal-free oxidation of 2,7-di-tert-butylpyrene. *Green Chem.* **2020**, *22* (18), 5966−5971.

(23) Nannenga, B. L.; Gonen, T. The cryo-EM method microcrystal electron diffraction (MicroED). *Nat. Methods* **2019**, *16* (5), 369−379.

(24) Ascherl, L.; Sick, T.; Margraf, J. T.; Lapidus, S. H.; Calik, M.; Hettstedt, C.; Karaghiosoff, K.; Döblinger, M.; Clark, T.; Chapman, K. W.; Auras, F.; Bein, T. Molecular docking sites designed for the generation of highly crystalline covalent organic frameworks. *Nat. Chem.* **2016**, *8* (4), 310−316.

(25) Auras, F.; Ascherl, L.; Hakimioun, A. H.; Margraf, J. T.; Hanusch, F. C.; Reuter, S.; Bessinger, D.; Döblinger, M.; Hettstedt, C.; Karaghiosoff, K.; Herbert, S.; Knochel, P.; Clark, T.; Bein, T. Synchronized Offset Stacking: A Concept for Growing Large-Domain and Highly Crystalline 2D Covalent Organic Frameworks. *J. Am. Chem. Soc.* **2016**, *138* (51), 16703−16710.

(26) Martínez-Abadía, M.; Stoppiello, C. T.; Strutynski, K.; Lerma-Berlanga, B.; Martí-Gastaldo, C.; Saeki, A.; Melle-Franco, M.; Khlobystov, A. N.; Mateo-Alonso, A. A Wavy Two-Dimensional Covalent Organic Framework from Core-Twisted Polycyclic Aromatic Hydrocarbons. *J. Am. Chem. Soc.* **2019**, *141* (36), 14403−14410.

(27) Martínez-Abadía, M.; Strutyński, K.; Lerma-Berlanga, B.; Stoppiello, C. T.; Khlobystov, A. N.; Martí-Gastaldo, C.; Saeki, A.; Melle-Franco, M.; Mateo-Alonso, A. π-Interpenetrated 3D Covalent Organic Frameworks from Distorted Polycyclic Aromatic Hydrocarbons. *Angew. Chem., Int. Ed.* **2021**, *60* (18), 9941−9946.

(28) Saeki, A.; Koizumi, Y.; Aida, T.; Seki, S. Comprehensive Approach to Intrinsic Charge Carrier Mobility in Conjugated Organic Molecules, Macromolecules, and Supramolecular Architectures. *Acc. Chem. Res.* **2012**, *45* (8), 1193−1202.

(29) Gozalvez, C.; Zafra, J. L.; Saeki, A.; Melle-Franco, M.; Casado, J.; Mateo-Alonso, A. Charge transport modulation in pseudorotaxane 1D stacks of acene and azaacene derivatives. *Chem. Sci.* **2019**, *10* (9), 2743−2749.

(30) Carini, M.; Marongiu, M.; Strutyński, K.; Saeki, A.; Melle-Franco, M.; Mateo-Alonso, A. Hooking Together Sigmoidal Monomers into Supramolecular Polymers. *Angew. Chem., Int. Ed.* **2019**, *58* (44), 15788−15792.

(31) Martínez-Abadía, M.; Antonicelli, G.; Saeki, A.; Mateo-Alonso, A. Readily Processable Hole-Transporting Peropyrene Gels. *Angew. Chem., Int. Ed.* **2018**, *57* (27), 8209−8213.

(32) Martínez-Abadía, M.; Antonicelli, G.; Saeki, A.; Melle-Franco, M.; Mateo-Alonso, A. Isolation and Characterization of the Unexpected 1-n-Octyloxyperopyrene: A Solution-Processable p-Type Organic Semiconductor. *J. Org. Chem.* **2019**, *84* (6), 3270−3274.

(33) Dalapati, S.; Addicoat, M.; Jin, S.; Sakurai, T.; Gao, J.; Xu, H.; Irle, S.; Seki, S.; Jiang, D. Rational design of crystalline supermicroporous covalent organic frameworks with triangular topologies. *Nat. Commun.* **2015**, *6*, 7786.

(34) Ding, H.; Li, Y.; Hu, H.; Sun, Y.; Wang, J.; Wang, C.; Wang, C.; Zhang, G.; Wang, B.; Xu, W.; Zhang, D. A Tetrathiafulvalene-Based Electroactive Covalent Organic Framework. *Chem.—Eur. J.* **2014**, *20* (45), 14614−14618.

(35) Jin, S.; Sakurai, T.; Kowalczyk, T.; Dalapati, S.; Xu, F.; Wei, H.; Chen, X.; Gao, J.; Seki, S.; Irle, S.; Jiang, D. Two-Dimensional Tetrathiafulvalene Covalent Organic Frameworks: Towards Latticed Conductive Organic Salts. *Chem.—Eur. J.* **2014**, *20* (45), 14608−14613.

https://doi.org/10.1021/jacs.2c06446
J. Am. Chem. Soc. 2022, 144, 15443−15450

(36) Wan, S.; Gándara, F.; Asano, A.; Furukawa, H.; Saeki, A.; Dey, S. K.; Liao, L.; Ambrogio, M. W.; Botros, Y. Y.; Duan, X.; Seki, S.; Stoddart, J. F.; Yaghi, O. M. Covalent Organic Frameworks with High Charge Carrier Mobility. *Chem. Mater.* **2011**, *23* (18), 4094−4097.
(37) Feng, X.; Chen, L.; Honsho, Y.; Saengsawang, O.; Liu, L.; Wang, L.; Saeki, A.; Irle, S.; Seki, S.; Dong, Y.; Jiang, D. An Ambipolar Conducting Covalent Organic Framework with Self-Sorted and Periodic Electron Donor-Acceptor Ordering. *Adv. Mater.* **2012**, *24* (22), 3026−3031.
(38) Feng, X.; Liu, L.; Honsho, Y.; Saeki, A.; Seki, S.; Irle, S.; Dong, Y.; Nagai, A.; Jiang, D. High-Rate Charge-Carrier Transport in Porphyrin Covalent Organic Frameworks: Switching from Hole to Electron to Ambipolar Conduction. *Angew. Chem., Int. Ed.* **2012**, *51* (11), 2618−2622.
(39) Ding, X.; Feng, X.; Saeki, A.; Seki, S.; Nagai, A.; Jiang, D. Conducting metallophthalocyanine 2D covalent organic frameworks: the role of central metals in controlling π-electronic functions. *Chem. Commun.* **2012**, *48* (71), 8952−8954.
(40) Ding, X.; Guo, J.; Feng, X.; Honsho, Y.; Guo, J.; Seki, S.; Maitarad, P.; Saeki, A.; Nagase, S.; Jiang, D. Synthesis of Metallophthalocyanine Covalent Organic Frameworks That Exhibit High Carrier Mobility and Photoconductivity. *Angew. Chem., Int. Ed.* **2011**, *50* (6), 1289−1293.
(41) Ding, X.; Chen, L.; Honsho, Y.; Feng, X.; Saengsawang, O.; Guo, J.; Saeki, A.; Seki, S.; Irle, S.; Nagase, S.; Parasuk, V.; Jiang, D. An n-Channel Two-Dimensional Covalent Organic Framework. *J. Am. Chem. Soc.* **2011**, *133* (37), 14510−14513.
(42) Thomas, S.; Li, H.; Dasari, R. R.; Evans, A. M.; Castano, I.; Allen, T. G.; Reid, O. G.; Rumbles, G.; Dichtel, W. R.; Gianneschi, N. C.; Marder, S. R.; Coropceanu, V.; Brédas, J.-L. Design and synthesis of two-dimensional covalent organic frameworks with four-arm cores: prediction of remarkable ambipolar charge-transport properties. *Mater. Horiz.* **2019**, *6* (9), 1868−1876.
(43) Martínez-Abadía, M.; Strutyński, K.; Stoppiello, C. T.; Lerma Berlanga, B.; Martí-Gastaldo, C.; Khlobystov, A. N.; Saeki, A.; Melle-Franco, M.; Mateo-Alonso, A. Understanding charge transport in wavy 2D covalent organic frameworks. *Nanoscale* **2021**, *13* (14), 6829−6833.
(44) Weare, B. L.; Lodge, R. W.; Zyk, N.; Weilhard, A.; Housley, C. L.; Strutyński, K.; Melle-Franco, M.; Mateo-Alonso, A.; Khlobystov, A. N. Imaging and analysis of covalent organic framework crystallites on a carbon surface: a nanocrystalline scaly COF/nanotube hybrid. *Nanoscale* **2021**, *13* (14), 6834−6845.
(45) Riaño, A.; Strutyński, K.; Liu, M.; Stoppiello, C. T.; Lerma-Berlanga, B.; Saeki, A.; Martí-Gastaldo, C.; Khlobystov, A. N.; Valenti, G.; Paolucci, F.; Melle-Franco, M.; Mateo-Alonso, A. An Expanded 2D Fused Aromatic Network with 90-Ring Hexagons. *Angew. Chem., Int. Ed.* **2022**, *61* (2), No. e202113657.

https://doi.org/10.1021/jacs.2c06446
J. Am. Chem. Soc. 2022, 144, 15443−15450